

## Structure and Absolute Configuration of Secondary Metabolites from Two Strains of *Streptomyces chartreusis* Associated with Attine Ants

Humberto E. Ortega,<sup>id a</sup> João M. Batista Jr.,<sup>id \*,b,c</sup> Weilan G. P. Melo,<sup>id a</sup>  
Gabriela T. de Paula<sup>a</sup> and Mônica T. Pupo<sup>id \*,a</sup>

<sup>a</sup>Faculdade de Ciências Farmacêuticas de Ribeirão Preto (FCFRP),  
Universidade de São Paulo (USP), 14040-903 Ribeirão Preto-SP, Brazil

<sup>b</sup>Departamento de Química, Universidade Federal de São Carlos (UFSCar),  
13565-905 São Carlos-SP, Brazil

<sup>c</sup>Instituto de Ciência e Tecnologia, Universidade Federal de São Paulo (UNIFESP),  
12231-280 São José dos Campos-SP, Brazil

The antibiotic streptazolin (**1**), its *E*-isomer (**2**), along with the stereoisomers strepachazolin A (**3**) and strepachazolin B (**4**) and the inorganic compound cyclooctasulfur (**5**) were produced in solid culture by *Streptomyces chartreusis* ICBG377, which was isolated from the fungal garden of the leaf-cutter ant *Acromyrmex subterraneus brunneus*. This is the first time compound **2** is reported as a natural product. Compound **5**, which showed antagonist activity against the specialized pathogenic fungus *Escovopsis* sp., was also produced by *Streptomyces chartreusis* ICBG323, isolated from the exoskeleton of winged male of *Mycocepurus goeldii*. The absolute configurations of **3** and **4** were confirmed by the combination of vibrational circular dichroism (VCD) spectroscopy and density functional theory (DFT) calculations. These results clearly demonstrate the power of VCD to tell apart epimeric natural products. Compounds **1**, **3** and **4** were produced by geographically distant but phylogenetically close strains, *S. chartreusis* ICBG 377 isolated in Brazil, and *S. chartreusis* NA02069, a marine sediment strain isolated in China.

**Keywords:** *Acromyrmex subterraneus brunneus*, *Mycocepurus goeldii*, leaf-cutter ant, strepachazolins A and B, VCD, DFT

### Introduction

Fungus-growing ants (tribe Attini) comprise more than 230 species, all of which depend on the cultivation of fungal gardens for food. They can be divided into five distinct agricultural systems: lower agriculture; coral fungus agriculture; yeast agriculture; generalized higher agriculture; and leaf-cutter agriculture that has evolved more recently to become the dominant herbivores of the New World tropics. The leaf-cutter agriculture involves different species of the two major genera, *Atta* and *Acromyrmex*, with the ability to cut and process fresh vegetation as a nutritional substrate for their fungal crop.<sup>1</sup> *Atta* and *Acromyrmex* are considered the highly evolved attines while lower attines comprise several genera including *Mycocepurus*, *Myrmicocrypta*, *Apterostigma*, *Mycetophylax*, *Mycetarotes*,

*Mycetosoritis*, and *Cyphomyrmex*, which retain more primitive features.<sup>1-3</sup>

Several new and known biologically active compounds have been identified from actinobacteria (*Streptomyces* and *Pseudonocardia*) isolated from fungus-growing ant colonies.<sup>4-7</sup> The first example was the new cyclic depsipeptide dentigerumycin, produced by the symbiotic *Pseudonocardia* sp., isolated from the exoskeleton of the coral fungus agriculture ant *Apterostigma dentigerum*. This compound has a selective inhibition against the specialized pathogenic fungus *Escovopsis* sp., found only in fungus-growing ants colonies, and also a potent inhibitory activity against several *Candida albicans* strains.<sup>8</sup> As part of the International Cooperative Biodiversity Group Program in Brazil (ICBG-Brazil),<sup>9</sup> we have investigated the small molecules produced by *Streptomyces chartreusis* ICBG377, isolated from the fungal garden of the leaf-cutter ant *Acromyrmex subterraneus brunneus*; and from

\*e-mail: batista.junior@unifesp.br; mtpupo@fcrfp.usp.br

*Streptomyces chartreusis* ICBG323, isolated from the exoskeleton of winged males of *Mycocephalus goeldii*. *S. chartreusis* ICBG377 produced streptazolin (**1**), its *E*-isomer (**2**), strepchazolin A (**3**), strepchazolin B (**4**) and cyclooctasulphur (**5**) (Figure 1); while compound **5** was also produced by *S. chartreusis* ICBG323. It is noteworthy that this is the first time compound **2** is reported as a natural product.

In this paper, besides reporting the isolation and structural characterization of compounds **1-5**, we describe the use of vibrational circular dichroism (VCD) spectroscopy and density functional theory (DFT) calculations to confirm the absolute configuration of the stereoisomers **3** and **4**. The unambiguous assignment of absolute configuration is a common bottleneck in the natural product isolation pipeline,<sup>10</sup> especially when epimers are concerned. Finally, the possible ecological function of **5** in fungus-growing ant ecosystems is also discussed.

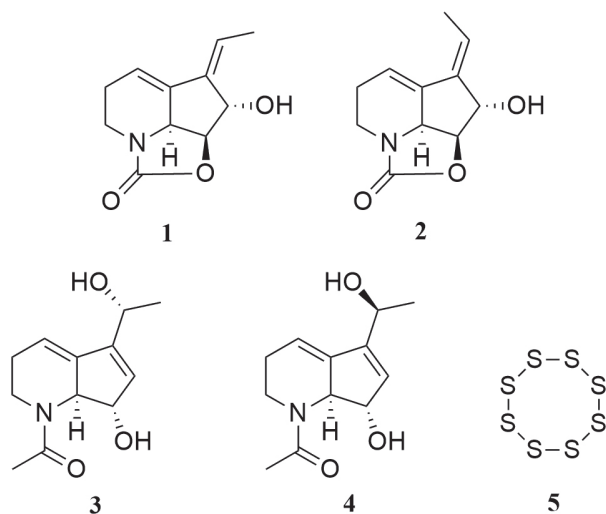


**Figure 1.** Compounds isolated from *Streptomyces chartreusis* ICBG377.

## Results and Discussion

Strain ICBG377 was isolated from the fungal garden of *Acromyrmex subterraneus brunneus* and strain ICBG323 was isolated from winged male *Mycocephalus goeldii*. Both strains were identified by 16S rRNA sequencing as *Streptomyces chartreusis*. Several antitumor and antibiotics compounds have been reported from soil *S. chartreusis* strains, such as cephamycins SF-1623 and SF-1623B; chartreusin, chrymutasins, calcimycin, cezomycin, and others.<sup>11-14</sup> *S. chartreusis* ICBG377 and ICBG323 inhibited the growth of *Escovopsis* sp. in antagonism bioassays (Figures S1 and S2, respectively, Supplementary Information (SI) section). Therefore, strains ICBG377 and ICBG323 were grown on ISP-2 agar, and the cultures were extracted with EtOAc for chemical studies.

The two major compounds detected by high-performance liquid chromatography ultraviolet detector (HPLC-UV) from the ethyl acetate (EtOAc) extract of *S. chartreusis* ICBG377 were streptazolin (**1**) and its *E*-isomer (**2**) (Figure S3, SI section). They were identified by comparison of their nuclear magnetic resonance (NMR) and mass spectrometry (MS) data with that in the literature (Figures S4-S7, SI section).<sup>15,16</sup> Compound **1** has only been isolated from the genus *Streptomyces*. It is an unusual antibiotic and antifungal compound,<sup>15</sup> which possesses its major structural features composed by a 1,2,5,6-tetrahydropyridine ring system, a cyclourethane, and an exocyclic ethylidene side chain.<sup>17</sup> Structural variants of streptazolin (**1**) such as 3,9-dihydrostreptazolin and Diels-Alder adducts with naphthoquinones show enhanced antimicrobial and cytotoxic activity.<sup>18</sup> Recent studies have found that streptazolin increases bacterial killing and the elaboration of immunostimulatory cytokines by macrophages *in vitro*.<sup>19</sup> The *E*-isomer of streptazolin (**2**) has been reported as an undesired side product in the synthesis of the streptazolin;<sup>17</sup> however, it had not been previously reported as a natural product.

Compound **3** gave a peak in the high-resolution electrospray ionization mass spectrometry (HRESIMS) consistent with a molecular formula  $C_{12}H_{17}NO_3$  (Figure S8, SI section). The UV and NMR data of **3** (Table 1 and Figures S9-S13, SI section) indicated that it is strepchazolin A.<sup>20</sup> Compound **3** does not contain the cyclourethane ring as observed in **1**. Instead, compound **3** has an acetyl group bound to the nitrogen atom, two hydroxyl groups at C-6 and C-9, and a double bond between C-7 and C-8. Both compounds **3** and **1** have a double bond between C-3 and C-4 (NMR data comparison in Table 1).

Compound **4** gave the same peak in the HRESIMS as observed for **3** (Figure S14, SI section). The UV and NMR data obtained for **4** are very similar to that of **3** (Table 1 and Figures S15-S23, SI section). There are small differences in hydrogen and carbon chemical shifts between **3** and **4**: H-3 ( $\delta_H$  6.01 for **3** and  $\delta_H$  5.90 for **4**), C-3 ( $\delta_C$  115.8 for **3** and  $\delta_C$  115.3 for **4**), C-7 ( $\delta_C$  131.0 for **3** and  $\delta_C$  129.8 for **4**), C-8 ( $\delta_C$  146.2 for **3** and  $\delta_C$  146.7 for **4**) and C-10 ( $\delta_C$  21.9 for **3** and  $\delta_C$  22.6 for **4**). Gradient-selected correlation spectroscopy (gCOSY) and gradient-selected heteronuclear multiple bond coherence (gHMBC) correlations observed for **4** were identical to those observed for **3**, indicating that it is strepchazolin B.<sup>20</sup>

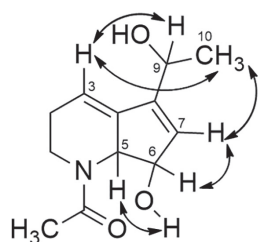
The relative configurations of compounds **3** and **4** were determined by nuclear Overhauser spectroscopy (NOESY) experiments. The key nuclear Overhauser effect (NOE) correlations are presented in Figure 2. Hydrogen H-5

**Table 1.**  $^1\text{H}$  (500 MHz) and  $^{13}\text{C}$  NMR (100 MHz) data for strepchazolin A (**3**) and strepchazolin B (**4**) ( $\text{CDCl}_3$ ) compared to NMR data for streptazolin (**1**) ( $\text{CDCl}_3$ )

Position	Strepchazolin A ( <b>3</b> ) <sup>a</sup>		Strepchazolin B ( <b>4</b> ) <sup>a</sup>		Streptazolin ( <b>1</b> ) <sup>b 17</sup>	
	$\delta_{\text{C}}$ / ppm, type	$\delta_{\text{H}}$ / ppm, mult. (J / Hz)	$\delta_{\text{C}}$ / ppm, type	$\delta_{\text{H}}$ / ppm, mult. (J / Hz)	$\delta_{\text{C}}$ / ppm, type	$\delta_{\text{H}}$ / ppm, mult. (J / Hz)
1	45.1, CH <sub>2</sub>	3.17, td (11.3, 3.9) 3.72, dt (12.0, 3.6)	45.1, CH <sub>2</sub>	3.16, td (11.2, 3.8) 3.71, dt (12.0, 3.6)	39.9, CH <sub>2</sub>	3.36-3.51, m
2	25.2, CH <sub>2</sub>	2.31, m	25.2, CH <sub>2</sub>	2.28, m	22.8, CH <sub>2</sub>	2.13-2.25, m 2.51, dtd (16.7, 7.2, 3.3)
3	115.8, CH	6.01, quint (3.4)	115.3, CH	5.90, m	118.9, CH	6.02-6.07, m
4	140.2, C	–	140.5, C	–	142.8, C	–
5	67.5, CH	4.35, br s	67.5, CH	4.34, br s	59.1, CH	4.26-4.31, m
6	79.8, CH	4.61, br s	79.8, CH	4.60, br s	81.5, CH	4.73, d (6.8)
7	131.0, CH	5.96, br s	129.8, CH	5.98, br s	74.5, CH	4.88, br s
8	146.2, C	–	146.7, C	–	139.1, C	–
9	64.5, CH	4.58, m	64.7, CH	4.58, m	123.7, CH	6.15, q (7.3)
10	21.9, CH <sub>3</sub>	1.44, d (6.42)	22.6, CH <sub>3</sub>	1.41, d (6.56)	14.9, CH <sub>3</sub>	1.91, d (7.3)
11	173.0, C	–	172.9, C	–	159.3, C	–
12	23.1, CH <sub>3</sub>	2.19, s	23.2, CH <sub>3</sub>	2.18, s	–	–
6-O-H	–	5.86, s	–	5.86, s	–	–

<sup>a</sup>NMR data previously published for **3** and **4** were recorded in  $\text{CD}_3\text{OD}$ ; <sup>20</sup><sup>b</sup> $^1\text{H}$  (400 MHz) and  $^{13}\text{C}$  NMR (100.6 MHz) data for **1** obtained in  $\text{CDCl}_3$ ;  $^1\text{H}$  NMR data for **3** and **4** were acquired in a DRX-500 Bruker spectrometer and  $^{13}\text{C}$  NMR data in a DRX-400 Bruker spectrometer in our experiments.

presents a correlation with the hydrogen of the hydroxyl group at C-6 in both compounds, indicating that they are on the same face of the molecules. Therefore, their absolute configuration could be only *5S,6S* or *5R,6R*. Compounds **3** and **4** also share other common NOE correlations: H-3 and H-9, H-3 and H-10, as well as between H-10 and H-7 (Figures S13 and S23, SI section). Based on that, compounds **3** and **4** are concluded to be epimers at C-9. The different arrangement of the substituents at C-9 accounts for the distinct chemical shifts of H-3, C-3, C-7, C-8 and C-10 in both compounds. Compounds **3** and **4** presented different retention times in HPLC analysis (see Figure S3, SI section), reinforcing that they are stereoisomers. Strepchazolin B (**4**) eluted first than strepchazolin A (**3**) using C<sub>6</sub>-Phenyl HPLC column.

**Figure 2.** Key NOE correlations of compounds **3** and **4**.

Once the planar structures of **3** and **4** were elucidated, we proceeded with attempts to assign their absolute

configurations. To that end, experimental infrared (IR)/VCD spectra were recorded for both compounds in methanol-*d*<sub>4</sub>, which were then compared to the theoretical data obtained for both diastereoisomers possible. The comparison between observed and calculated spectra at the B3PW91/PCM(MeOH)/6-311G(d,p) level (Figure 3) allowed for the unambiguous determination of the absolute configuration of compound (–)-**3** as (*5S,6S,9R*) and (–)-**4** as (*5S,6S,9S*). Despite the high degree of similarity between the IR and VCD spectra of **3** and **4**, the VCD band at around 1385 cm<sup>-1</sup>, which presented opposite signs for both epimers and was consistently reproduced by the calculations, represented the key spectral marker considered for these assignments. This band arises predominantly from the in-plane bending of H-9 coupled with the symmetrical bending of the methyl group at C-10, as well as with the C–C stretches between C-4/C-8 and C-8/C-9. The fact that these particular vibrations involve the atoms directly linked to chiral center at C-9 provides a higher level of confidence for this assignment. The lowest-energy conformers identified for both configurations at C-9 (Figure 4) also help explain most of the above-mentioned NMR data, such as the NOE correlations that are common to both **3** and **4**. Interestingly, for strepchazolin A (**3**) the OH group points predominantly towards H-3, while for strepchazolin B (**4**) the same group at C-9 points away from H-3 for most conformers. These findings may be responsible for the small difference in

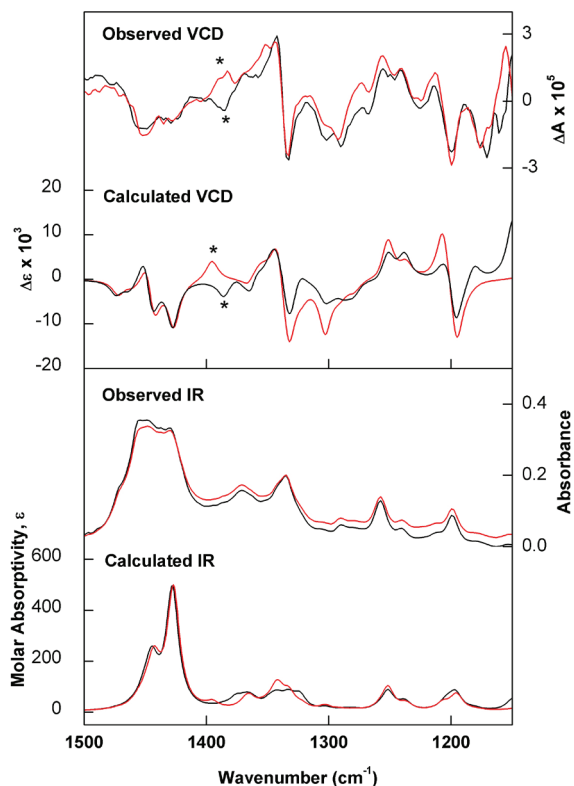


**Figure 3.** Comparison of the observed IR and VCD spectra of (–)-**3** (black trace) and (–)-**4** (red trace) with the calculated (B3PW91/PCM(MeOH)/6-311G(d,p)) IR and VCD spectra of the Boltzmann average of the four lowest-energy conformers identified for streptchazolin A (black trace) and streptchazolin B (red trace). The asterisks represent the key VCD bands considered for the assignment of (–)-**3** as (5*S*,6*S*,9*R*) and (–)-**4** as (5*S*,6*S*,9*S*).

the chemical shift observed for H-3 in both epimers due to the deshielding anisotropic effect of the oxygen lone-pairs. The absolute configurations of **3** and **4** were recently determined by X-ray and Mosher's method, respectively,<sup>20</sup> and our VCD data are in agreement with the previously established stereochemistry.

The wealth of structural and conformational information obtained from vibrational spectroscopy combined with the extra sensitivity to molecular chirality provided by VCD has made the latter a valuable new addition to the natural product chemistry toolbox.<sup>21</sup>

Cyclooctasulfur (**5**) was identified as the major compound by gas chromatography-mass spectrometry (GC-MS) (Figures S24-S25, SI section) from the unique bioactive fractions of both *S. chartreusis* strains (ICBG377 and ICBG323) against *Escovopsis* sp. (Figures S26-S27, SI section). Compound **5** has been previously reported from the North Sea *Streptomyces* GWS-BW-H5.<sup>22</sup> Under normal conditions, sulfur atoms form cyclic octatomic molecules. The element sulfur has been used as antimicrobial agent, insecticide, fumigant, etc.<sup>23</sup> So, *S. chartreusis* ICBG377 and ICBG323 could use **5** to help in the growth control of the pathogenic fungus *Escovopsis*. Compounds **1-4** did not show antifungal activity against *Escovopsis*.

Streptazolin (**1**), streptchazolin A (**3**) and streptchazolin B (**4**) were reported recently from *S. chartreusis* NA02069 (MH540322) isolated from marine sediment.<sup>20</sup> Compound **3** was published with weak

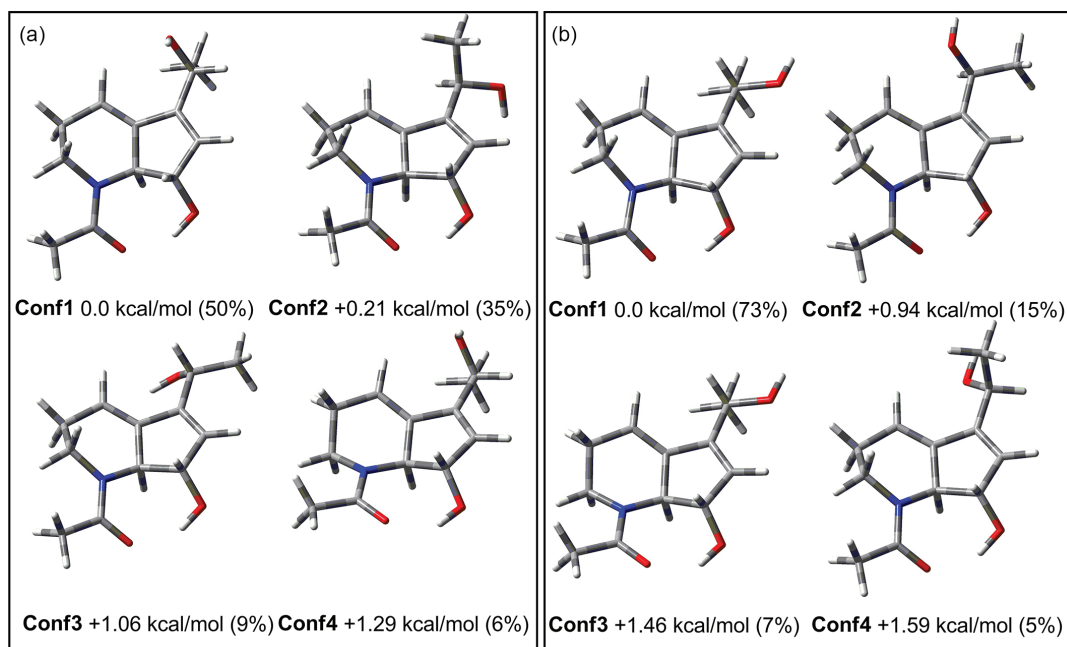


**Figure 4.** (a) Structures, relative Gibbs free energies (referenced to Conf1,  $G = -469127.091$  kcal mol<sup>-1</sup>), and Boltzmann population (%) of the four lowest-energy conformers of streptchazolin A (**3**) at the B3PW91/PCM(MeOH)/6-311G(d,p) level. (b) Structures, relative Gibbs free energies (referenced to Conf1,  $G = -469126.203$  kcal mol<sup>-1</sup>), and Boltzmann population (%) of the four lowest-energy conformers of streptchazolin B (**4**) at the B3PW91/PCM(MeOH)/6-311G(d,p) level.

anti-*Bacillus subtilis* activity with minimal inhibitory concentration (MIC) value of 64.0  $\mu\text{M}$ , and weak inhibitory activity against acetylcholinesterase (AChE) *in vitro* with half maximal inhibitory concentration ( $\text{IC}_{50}$ ) value of 50.6  $\mu\text{M}$ , while compound **4** was almost inactive.<sup>20</sup>

A phylogenetic tree was constructed and included 24 strains of the genus *Streptomyces* from databases, two ant-associated *S. chartreusis* (ICBG377 and ICBG323) from our study and rooted with *Nocardioopsis prasina* (Figure 5). The phylogenetic tree revealed that *S. chartreusis* strains ICBG377 and ICBG323 are clustering close to the other five *S. chartreusis* strains (MH540322, HQ400614, NR114825, NR041216 and HQ398415), which were isolated from marine sediment, soil and marine sponge. Interestingly, compounds **1**, **3** and **4** were produced by two geographically distant but phylogenetically close *S. chartreusis* strains, ICBG 377 isolated from ants in Brazil, and NA02069 isolated from marine sediment in China.

## Conclusions

*Streptomyces chartreusis* ICBG377 produced streptazolin (**1**), its *E*-isomer (**2**), strepachazolin A (**3**), strepachazolin B (**4**) and cyclooctasulphur (**5**); while compound **5** was also produced by *S. chartreusis* ICBG323. The absolute configurations of **3** and **4** were unambiguously confirmed as 5*S*,6*S*,9*R* and 5*S*,6*S*,9*S*, respectively, by means of VCD and DFT calculations, in agreement with recent data using X-ray crystallography and Mosher's analysis. In our study, the vibrational chiroptical spectroscopic analyses were carried out directly in solution and without the need of either single crystals or derivatizations, showing the advantage of VCD for the establishment of stereochemistry. The phylogenetic analysis corroborates that geographically distant bacterial strains can encode the same biosynthetic gene clusters for the production of natural products. The inorganic compound **5** was found to be the chemical defense

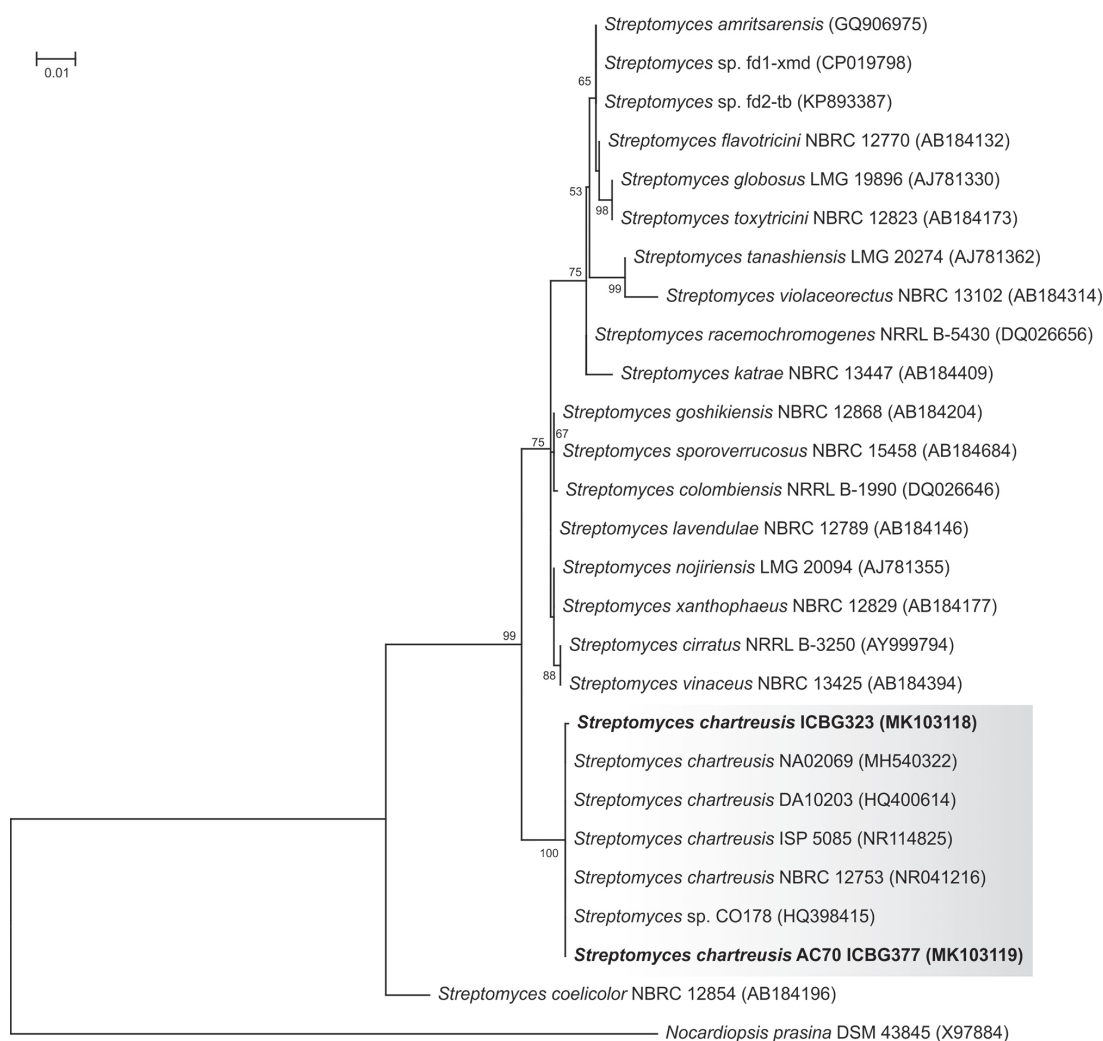


**Figure 5.** Phylogenetic tree including *S. chartreusis* strains (ICBG377 and ICBG323) based on 16S rRNA sequence. Scale bar represents 0.01 substitutions per site.

produced by both *S. chartreusis* strains to control the growth of the specialized pathogenic fungus *Escovopsis* sp. Compound **5** has been previously reported from a marine *Streptomyces* and is the most common allotrope of sulfur found in nature. The element sulfur has been demonstrated as antimicrobial agent, therefore this corroborates the antifungal activity of **5** against *Escovopsis*.

## Experimental

### General experimental procedures

A HPLC system (Shimadzu, Kyoto, Japan) equipped with an LC-6AD solvent pump, an SCL 10AVB system controller, a CTO-10ASVP column oven, a Rheodyne model 7725 injector, an SPD-M10AVP diode array detector, a Class VP software for data acquisition, and an analytical column (Phenomenex, C6-Phenyl, 5  $\mu\text{m}$ , 250  $\times$  4.6 mm). The HPLC purification were carried out at 3-6 mL min<sup>-1</sup> with a reversed-phase C6-phenyl semipreparative column (Phenomenex, C6-Phenyl, 5  $\mu\text{m}$ , 250  $\times$  10 mm) using aqueous acetonitrile (ACN). Specific optical rotations were recorded in a P-2000 digital polarimeter (Jasco, Tokyo, Japan). The mass spectrometry data were acquired with a UPLC (Shimadzu) coupled to a micrOTOF II mass spectrometer (Bruker Daltonics). One- and two-dimensional NMR spectra were recorded with 500 MHz (DRX-500) and 400 MHz (DRX-400) spectrometers (Bruker UK, Coventry, UK) using deuterated chloroform, referenced to the internal solvent peak at  $\delta_{\text{H}}$  7.26 and  $\delta_{\text{C}}$  77.16. All solvents used in the study were of research grade quality or better. IR and VCD spectra of **3** and **4** were recorded with a Single-PEM Chiral IR-2X FT-VCD spectrometer (BioTools, Inc., Jupiter, USA) using a resolution of 4 cm<sup>-1</sup> and a collection time of 8 h. The optimum retardation of the ZnSe photoelastic modulator (PEM) was set at 1400 cm<sup>-1</sup>. Minor instrumental baseline offsets were eliminated from the final VCD spectrum by subtracting the VCD spectrum of each compound from that of the solvent obtained under identical conditions. The IR and VCD spectra were recorded in a BaF<sub>2</sub> cell with 100  $\mu\text{m}$  path length using methanol-*d*<sub>4</sub> as solvent. Samples were prepared using 5 mg of each compound dissolved in 140  $\mu\text{L}$  of solvent. The gas chromatography spectrum of **5** was recorded in a gas chromatograph-mass spectrometer (Shimadzu, Kyoto, Japan).

### Isolation and cultivation of bacteria

Collection of biological samples and research was authorized by Brazilian government (SISBIO authorization 46555-6, CNPq process 010936/2014-

9). Samples of the fungal garden of *Acromyrmex subterraneus brunneus* were collected in Ribeirão Preto, São Paulo state, Brazil (S 21°10'13.0"; W 47°50'49.4"; W-47.8470555556; S-21.1702777778), on August 2014; and winged males of *Mycocepurus goeldii* were collected in same region (S 21°09'50.4"; W 47°50'56.0"; W-47.848889; S-21.163889), on October 2015. The bacterial strain ICBG377 was isolated by vortexing small pieces of fungal garden of *Acromyrmex subterraneus brunneus* colony in 750  $\mu\text{L}$  of sterile deionized water, and subsequently spreading 100  $\mu\text{L}$  of this suspension onto chitin-agar plates containing antifungal (0.05 g cycloheximide *per* liter of medium, and 0.04 g nystatin dissolved in dimethyl sulfoxide (DMSO)); while strain ICBG323 was isolated by vortexing winged males of *Mycocepurus goeldii* in 500  $\mu\text{L}$  sterile deionized water, and subsequently spreading 100  $\mu\text{L}$  of this suspension onto same chitin-agar plates. After 2-4 weeks of growth at 30 °C, bacterial colonies were sub-cultured onto ISP-2-agar plates, and serial culturing was done until pure cultures were obtained.<sup>24</sup>

### DNA extraction for bacterial identification

Genomic DNA was extracted using a modified protocol.<sup>25</sup> Actinobacteria were grown in 4 mL of liquid medium ISP-2 at 30 °C for 72 h. After this period, the cultures were centrifuged at 5,000 g for 5 min. The supernatant was discarded, and the culture pellet transferred to a 2.0 mL Eppendorf tube with 500  $\mu\text{L}$  of TE buffer 0.01X. It was added 3  $\mu\text{L}$  of RNase to digest the RNA and then added 400  $\mu\text{L}$  of solution I (1% Sarkosyl, 0.5 M NaCl, 1% sodium dodecyl sulfate (SDS)). The tubes were kept for 10 min at 37 °C with continuous stirring. Then, 400  $\mu\text{L}$  of phenol:chloroform:isoamyl alcohol, 25:24:1 (PCI) were added and mixed by inversion and centrifuged at 10,000 g for 5 min at 37 °C, followed by carefully transferring the supernatant to a new 1.5 mL Eppendorf tube. Then, 10% of the total volume of sodium acetate (3 M, pH 5.2) and 60% isopropanol were added and gently mixed by inverting tube 5 to 10 times. Then the tubes were centrifuged for 5 min at 10,000 g at 37 °C. The DNA was precipitated in the pellet and the liquid removed. The pellet was washed with 1 mL of 70% ethanol and centrifuged at 10,000 g for 3 min at 37 °C. The supernatant was removed and the DNA after dried was resuspended in 20  $\mu\text{L}$  of TE 0.01X.

### Amplification - polymerase chain reaction (PCR)

The 16S rRNA gene was amplified from genomic DNA by polymerase chain reaction (PCR) using a pair of universal primers F27 (5'-AGAGTTTGTATCATGGCTCAG-3') and

R1492 (5'-TACGGTTACCTTGTACGACTT-3').<sup>26</sup> The PCR reactions contained 2  $\mu\text{L}$  of DNA (10  $\text{ng } \mu\text{L}^{-1}$ ), 2.0  $\mu\text{L}$  of each primer (10  $\mu\text{M}$ ), 2.5  $\mu\text{L}$  of 10X buffer, 2.0  $\mu\text{L}$  of  $\text{MgCl}_2$  (25 mM), 4.0  $\mu\text{L}$  of dNTPs (1.25 mM each base), 0.2  $\mu\text{L}$  taq-polymerase (5 U  $\mu\text{L}^{-1}$ ) and 10.3  $\mu\text{L}$  of sterile milli-Q water for a total volume of 25.0  $\mu\text{L}$ . PCR was performed in a thermocycler (Applied Biosystems), in which amplification conditions were initiated by denaturation step with one cycle at 95 °C for 3 min, followed by an annealing step and extension in 35 cycles at 95 °C for 1 min, 60 °C for 1 min and 72 °C for 2 min and a final extension cycle at 72 °C for 15 min, and maintained at 10 °C. Amplification products were subjected to agarose gel electrophoresis 1% in 1X TBE buffer and stained with GelRed® (Biotium, Fremont, USA). Purification was performed with ethylenediaminetetraacetic acid (EDTA)-ethanol.

#### Amplification and purification of sequencing reaction

The same primers F27 and R1492 and the inner primer U519F (5'-CAGCMGCCGCGGTAATWC-3') were used for the sequencing reaction of 16S rRNA gene. The reactions containing 2.0  $\mu\text{L}$  5X buffer, 0.32  $\mu\text{L}$  of primer (10  $\mu\text{M}$ ), 0.3  $\mu\text{L}$  of BigDye® 3.1 (Applied Biosystems, Waltham, USA), about 20 ng of purified DNA and sterile Milli-Q water to complete a total volume of 10  $\mu\text{L}$ . The thermocycler program consisted of 28 cycles at 95 °C for 15 s, followed by 50 °C for 45 s and 60 °C for 4 min, being completed and maintained at 10 °C. The sequencing reaction was purified according to the instructions in the manual BigDye® (Applied Biosystems, Waltham, USA).

#### Sequencing of the 16S rRNA gene and editing sequences

The sequencing was performed in equipment ABI 3500 (Applied Biosystems, Waltham, USA). Sequences were edited and used to assemble the contigs in BioEdit 7.2.5.<sup>27</sup> Contigs were used to search for homologous sequences in databases National Center for Biotechnology Information (NCBI) - GenBank<sup>28</sup> and Eztaxon.<sup>29</sup>

#### Phylogenetic analysis

Phylogenetic and molecular evolutionary analyses were conducted in MEGA version X,<sup>30</sup> using the maximum likelihood method based on the Tamura-Nei model and a discrete gamma distribution. The analysis involved 27 nucleotide sequences including *S. chartreusis* ICBG323 and ICBG377 and was rooted by *Nocardiopsis prasina*. All positions containing gaps and missing data were eliminated.

There were a total of 1342 positions in the final dataset. The DNA sequences were deposited in the NCBI-GenBank under accession numbers MK103118 (ICBG323) and MK103119 (ICBG377).

#### Purification of compounds 1-5

Strain ICBG377 was grown on solid ISP-2 medium (*per liter*: yeast extract, 4 g; malt extract, 10 g; glucose, 4 g; agar, 20 g) in 151 Petri plates (140 × 20 mm, 10.7 L total) for 10 days at 30 °C. The solid agar was cut into small cubes and soaked three times in EtOAc overnight. The solvent was filtered and dried under vacuum to give the crude extract (3.3 g). The extract was dissolved in 90% MeOH:H<sub>2</sub>O (200 mL), decanted and dried to give two fractions: A (soluble, 1.802 g) and B (insoluble, 452.13 mg). Fraction A was purified by solid phase extraction (SPE)-C18 (55  $\mu\text{m}$ , 10 g/60 mL, Phenomenex, Torrance, USA) using the following gradient: 200 mL (10% MeOH:H<sub>2</sub>O, A1: 613.97 mg); 200 mL (20% MeOH:H<sub>2</sub>O, A2: 97.68 mg); 200 mL (40% MeOH:H<sub>2</sub>O, A3: 43.93 mg); 200 mL (60% MeOH:H<sub>2</sub>O, A4: 82.61 mg); 200 mL (80% MeOH:H<sub>2</sub>O, A5: 165.22 mg); 200 mL (100% MeOH, A6: 511.37 mg) and 200 mL (100% acetone, A7: 209.00 mg).

Fractions A1-A5 were combined and purified by semi-preparative HPLC using C<sub>6</sub>-Phenyl column (5  $\mu\text{m}$ , 250 × 10 mm) and the following gradient at 3 mL min<sup>-1</sup>: 0-5 min, isocratic flow of 5% CH<sub>3</sub>CN:H<sub>2</sub>O; 5-23 min, linear gradient from 5% CH<sub>3</sub>CN:H<sub>2</sub>O to 50% CH<sub>3</sub>CN:H<sub>2</sub>O; 23-24 min, linear gradient from 50% CH<sub>3</sub>CN:H<sub>2</sub>O to 100% CH<sub>3</sub>CN; 24-25 min, isocratic flow of 100 % CH<sub>3</sub>CN and 25-26 min, from 100% CH<sub>3</sub>CN to 5% CH<sub>3</sub>CN:H<sub>2</sub>O to give six fractions: C1 (9.4 mg), C2 (19.19 mg), C3 (25.66 mg), C4 (42.91 mg), C5 (7.29 mg), and C6 (58.74 mg).

Fraction C4 was purified by semi-preparative HPLC using C<sub>6</sub>-Phenyl column (5  $\mu\text{m}$ , 250 × 10 mm) and an isocratic flow of 10% CH<sub>3</sub>CN at 6 mL min<sup>-1</sup> to yield **1** (1.77 mg,  $t_R$  = 22.6 min) and **2** (4.47 mg,  $t_R$  = 24.8 min).

Fraction C2 was further purified by semi-preparative HPLC using C<sub>6</sub>-Phenyl column (5  $\mu\text{m}$ , 250 × 10 mm) and an isocratic flow of 10% CH<sub>3</sub>CN at 6 mL min<sup>-1</sup> to yield strepchazolin A (**3**) (3.60 mg,  $t_R$  = 18.4 min) and strepchazolin B (**4**) (3.49 mg,  $t_R$  = 16.7 min).

Fractions B, A6 and A7 showed activity against the *Escovopsis* sp. They were combined and purified by SPE-Si (55  $\mu\text{m}$ , 10 g/60 mL, Phenomenex, Torrance, USA) using the following gradient: 100 mL (100% hexane, B1: 280.38 mg); 100 mL (9:1 hexane:EtOAc, B2: 498.90 mg); 100 mL (8:2 hexane:EtOAc, B3: 85.72 mg); 100 mL (7:3 hexane:EtOAc,

B4: 22.14 mg); 100 mL (6:4 hexane:EtOAc, B5: 55.07 mg); 100 mL (1:1 hexane:EtOAc, B6: 7.33 mg); 100 mL (4:6 hexane:EtOAc, B7: 5.29 mg); 100 mL (2:8 hexane:EtOAc, B8: 5.62 mg); 100 mL (100% EtOAc, B9: 6.21 mg) and 100 mL (100% MeOH, B10: 117.44 mg). The fraction B1 was purified by solubility: B1.1 (soluble in acetone, 268.03 mg) and B1.2 (insoluble in acetone, 12.35 mg). All fractions obtained were tested against the *Escovopsis* sp. The fraction B1.2 was active (see Figure S26, SI section). Gas chromatography mass spectrometry (GC-MS) analysis of the active fraction B1.2 was carried out revealing cyclooctasulfur (**5**) as major compound (Figure S24, SI section).

Strain ICBG323 was also grown on solid ISP-2 medium. A similar protocol was used for fractionation of crude extract and identification of the cyclooctasulfur (**5**) by GC-MS (Figure S25, SI section) from active fraction against *Escovopsis*.

#### Computational methods

All density functional theory (DFT) calculations were carried out at 298 K in methanol solution using the polarizable continuum model (PCM) in its integral equation formalism version (IEFPCM) incorporated in Gaussian 09 software.<sup>31</sup> Calculations were performed for the arbitrarily chosen strepchazolin A (**3**) and strepchazolin B (**4**), as depicted in Figure 1. The conformational search was carried out at the molecular mechanics level of theory with the Monte Carlo algorithm employing the MM+ force field, incorporated in HyperChem 8.0.10 software.<sup>32</sup> Initially, for strepchazolin A (**3**), nine conformers with a relative energy (rel E.) within 6 kcal mol<sup>-1</sup> of the lowest-energy conformer were selected and geometry optimized at the B3LYP/PCM(MeOH)/6-31G(d) level. The conformers for strepchazolin B (**4**) were generated by inverting the configuration at C-9 for all conformers identified in the previous step for strepchazolin A (**3**). These conformers were then geometry optimized at the B3LYP/PCM(MeOH)/6-31G(d) level. Before IR and VCD calculations all conformers obtained for both diastereoisomers were further geometry optimized at the B3PW91/PCM(MeOH)/6-311G(d,p) level. The four conformers identified for each configuration with rel E. < 1.6 kcal mol<sup>-1</sup>, which corresponded to more than 97% of the total Boltzmann distributions, were considered for IR and VCD spectral calculations. In order to better reproduce experimental data recorded in methanol-*d*<sub>4</sub>, the input structures were created with exchangeable hydrogens replaced with deuterium atoms.<sup>33</sup> IR and VCD spectra were created using dipole and rotational

strengths from Gaussian, which were calculated at the B3PW91/PCM(MeOH)/6-311G(d,p) level, and converted into molar absorptivities (M<sup>-1</sup> cm<sup>-1</sup>). The Boltzmann factor for each conformer was calculated based on Gibbs free energies. Each spectrum was plotted as a sum of Lorentzian bands with half-widths at half-maximum of 6 cm<sup>-1</sup>. The calculated wavenumbers were multiplied with a scaling factor of 0.98 and the final Boltzmann-population-weighted composite spectra were plotted using Origin 8 software.<sup>34</sup>

#### Supplementary Information

NMR and HRMS spectra of compounds **1-4** and GC-MS spectra of **5** is available free of charge via the internet at <http://jbcs.sbq.org.br> as a PDF file.

#### Acknowledgments

The authors acknowledge the financial support from São Paulo Research Foundation (FAPESP) grants No. 2013/50954-0, No. 2014/14095-6, No. 2015/07089-2, No. 2014/25222-9, No. 2015/01001-6, and No. 2017/05920-1; and Conselho Nacional de Desenvolvimento Científico e Tecnológico (CNPq grant No. 307147/2014-2). This study was financed in part by the Coordenação de Aperfeiçoamento de Pessoal de Nível Superior - Brasil (CAPES) - Finance Code 001. We thank Dr Sandra Verza (Centro de Estudos de Insetos Sociais - UNESP-RC) for identification of the ants, Eduardo A. Silva Jr. and Lohan Valadares for helping fungal garden collection and Claudia C. de Macedo for technical assistance. This research was also supported by resources supplied by the Centre for Scientific Computing (NCC/GridUNESP) of the São Paulo State University (UNESP).

#### References

- Schultz, T. R.; Brady, S. G.; *Proc. Natl. Acad. Sci.* **2008**, *105*, 5435.
- Hölldobler, B.; Wilson, E. O.; *The Ants*, 1<sup>st</sup> ed.; Harvard University Press: Cambridge, 1990.
- Branstetter, M. G.; Ješovnik, A.; Sosa-Calvo, J.; Lloyd, M. W.; Faircloth, B. C.; Brady, S. G.; Schultz, T. R.; *Proc. R. Soc. B* **2017**, *284*, 1852.
- Carr, G.; Derbyshire, E. R.; Caldera, E.; Currie, C. R.; Clardy, J.; *J. Nat. Prod.* **2012**, *75*, 1806.
- Haeder, S.; Wirth, R.; Herz, H.; Spittler, D.; *Proc. Natl. Acad. Sci.* **2009**, *106*, 4742.
- Schoenian, I.; Spittler, M.; Ghaste, M.; Wirth, R.; Herz, H.; Spittler, D.; *Proc. Natl. Acad. Sci.* **2011**, *108*, 1955.



7. Mendes, T. D.; Borges, W. S.; Rodrigues, A.; Solomon, S. E.; Vieira, P. C.; Duarte, M. C. T.; Pagnocca, F. C.; *Biomed Res. Int.* **2013**, *2013*.
8. Oh, D. C.; Poulsen, M.; Currie, C. R.; Clardy, J.; *Nat. Chem. Biol.* **2009**, *5*, 391.
9. Pupo, M. T.; Currie, C. R.; Clardy, J.; *J. Braz. Chem. Soc.* **2017**, *28*, 393.
10. N. L. Batista, A.; Santos, F. M.; Batista, J.; Cass, Q. B.; *Molecules* **2018**, *23*, 492.
11. Aoyama, Y.; Katayama, T.; Yamamoto, M.; Tanaka, H.; Kon, K.; *J. Antibiot.* **1992**, *45*, 875.
12. David, L.; Kergomard, A.; *J. Antibiot.* **1982**, *35*, 1409.
13. Uchida, H.; Nakakita, Y.; Enoki, N.; Abe, N.; Nakamura, T.; Munekata, M.; *J. Antibiot.* **1994**, *47*, 655.
14. Wu, Q.; Liang, J.; Lin, S.; Zhou, X.; Bai, L.; Deng, Z.; Wang, Z.; *Antimicrob. Agents Chemother.* **2011**, *55*, 974.
15. Drautz, H.; Zähler, H.; Kupfer, E.; Keller-Schierlein, W.; *Helv. Chim. Acta* **1981**, *164*, 1752.
16. Li, F.; Warshakoon, N. C.; Miller, M. J.; *J. Org. Chem.* **2004**, *69*, 8836.
17. Yamada, H.; Aoyagi, S.; Kibayashi, C.; *J. Am. Chem. Soc.* **1996**, *118*, 1054.
18. Grabley, S.; Kluge, H.; Hoppe, H. U.; *Angew. Chem., Int. Ed. Engl.* **1987**, *26*, 664.
19. Perry, J. A.; Koteva, K.; Verschoor, C. P.; Wang, W.; Bowdish, D. M.; Wright, G. D.; *J. Antibiot.* **2015**, *68*, 40.
20. Yang, C. L.; Wang, Y. S.; Liu, C. L.; Zeng, Y. J.; Cheng, P.; Jiao, R. H.; Bao, S. X.; Huang, H. Q.; Tan, R. X.; Ge, H. M.; *Mar. Drugs* **2017**, *15*, 244.
21. Batista, J. M.; Blanch, E. W.; Silva, V. B.; *Nat. Prod. Rep.* **2015**, *32*, 1280.
22. Dickschat, J. S.; Martens, T.; Brinkhoff, T.; Simon, M.; Schulz, S.; *Chem. Biodivers.* **2005**, *2*, 837.
23. Deshpande, A. S.; Khomane, R. B.; Vaidya, B. K.; Joshi, R. M.; Harle, A. S.; Kulkarni, B. D.; *Nanoscale Res. Lett.* **2008**, *3*, 221.
24. Poulsen, M.; Currie, C. R.; *PLoS One* **2010**, *5*, e8748.
25. Sharma, A. D.; Singh, J.; *Anal. Biochem.* **2005**, *337*, 354.
26. Ludwig, W.; *Int. J. Food Microbiol.* **2007**, *120*, 225.
27. Hall, T. A.; *Nucleic Acids Symp. Ser.* **1999**, *41*, 95.
28. <https://blast.ncbi.nlm.nih.gov/Blast.cgi> accessed on August 8, 2019.
29. <https://www.ezbiocloud.net/taxonomy> accessed on August 8, 2019.
30. Kumar, S.; Stecher, G.; Li, M.; Knyaz, C.; Tamura, K.; *Mol. Biol. Evol.* **2018**, *35*, 1547.
31. Frisch, M. J.; Trucks, G. W.; Schlegel, H. B.; Scuseria, G. E.; Robb, M. A.; Cheeseman, J. R.; Scalmani, G.; Barone, V.; Mennucci, B.; Petersson, G. A.; Nakatsuji, H.; Caricato, M.; Li, X.; Hratchian, H. P.; Izmaylov, A. F.; Bloino, J.; Zheng, G.; Sonnenberg, J. L.; Hada, M.; Ehara, M.; Toyota, K.; Fukuda, R.; Hasegawa, J.; Ishida, M.; Nakajima, T.; Honda, Y.; Kitao, O.; Nakai, H.; Vreven, T.; Montgomery Jr., J. A.; Peralta, J. E.; Ogliaro, F.; Bearpark, M.; Heyd, J. J.; Brothers, E.; Kudin, K. N.; Staroverov, V. N.; Kobayashi, R.; Normand, J.; Raghavachari, K.; Rendell, A.; Burant, J. C.; Iyengar, S. S.; Tomasi, J.; Cossi, M.; Rega, N.; Millam, J. M.; Klene, M.; Knox, J. E.; Cross, J. B.; Bakken, V.; Adamo, C.; Jaramillo, J.; Gomperts, R.; Stratmann, R. E.; Yazyev, O.; Austin, A. J.; Cammi, R.; Pomelli, C.; Ochterski, J. W.; Martin, R. L.; Morokuma, K.; Zakrzewski, V. G.; Voth, G. A.; Salvador, P.; Dannenberg, J. J.; Dapprich, S.; Daniels, A. D.; Farkas, Ö.; Foresman, J. B.; Ortiz, J. V.; Cioslowski, J.; Fox, D. J.; *Gaussian 09, Revision A. 02*; Gaussian, Inc., Wallingford, USA, 2009.
32. *HyperChem 8.0.10*; Hypercube, Inc., Gainesville, USA, 2011.
33. Sprenger, R. F.; Thomasi, S. S.; Ferreira, A. G.; Cass, Q. B.; Batista Jr., J. M.; *Org. Biomol. Chem.* **2016**, *14*, 3369.
34. *Origin 8.0*; OriginLab, Northampton, USA, 2007.

Submitted: March 6, 2019

Published online: August 15, 2019

